Mon. Not. R. Astron. Soc. **306**, L31–L37 (1999)

Spectral evolution of magnetic flares and time lags in accreting black hole sources

Juri Poutanen[1,2]★ and Andrew C. Fabian[2]★

[1]*Stockholm Observatory, SE-133 36 Saltsjöbaden, Sweden*
[2]*Institute of Astronomy, Madingley Road, Cambridge CB3 0HA*

Accepted 1999 April 27. Received 1999 April 13; in original form 1998 November 23

ABSTRACT

We present a model for the short time-scale spectral variability of accreting black holes. It describes the time-averaged spectra well, and also temporal characteristics such as the power-density spectrum, time/phase lags, and coherence function of Cygnus X-1. We assume that X/γ-rays are produced in compact magnetic flares at radii $\lesssim 100GM/c^2$ from the central black hole. The tendency for magnetic loops to inflate and detach from the underlying accretion disc causes the spectrum of a flare to evolve from soft to hard because of the decrease of the feedback from the cold disc, so causing time delays between hard and soft photons. We identify the observed time lags with the evolution time-scales of the flares, which are of the order of the Keplerian time-scale. We model the overall temporal variability using a pulse avalanche model in which each flare has a certain probability of triggering a neighbouring flare, thus occasionally producing long avalanches. The duration of the avalanches determines the Fourier frequencies at which most of the power emerges.

Key words: accretion, accretion discs – radiation mechanisms: non-thermal – stars: flare – stars: individual: Cygnus X-1 – X-rays: general – X-rays: stars.

1 INTRODUCTION

The X-ray emission of many sources harbouring a black hole shows strong variability, on time-scales of milliseconds to hours for objects like Cygnus X-1 and other Galactic black holes (GBHs), and minutes to days for an active galaxy like MCG–6-30-15. The time-averaged spectra are often interpreted as the result of the Comptonization of soft photons in a hot static electron cloud (e.g. Shapiro, Lightman & Eardley 1976; Sunyaev & Trümper 1979). Surprisingly, even modern X/γ-ray data of one of the best-studied bright sources, Cyg X-1, are explained relatively well in terms of such models (Gierliński et al. 1997; Poutanen 1999; Zdziarski et al. 1998), despite the observed rapid variability. Detailed studies of the X-ray colours, however, have shown rapid spectral changes (Nolan et al. 1981; Negoro, Miyamoto & Kitamoto 1994), which imply the presence of rapid changes in the physical conditions of the source.

The properties of the observed variability are somewhat puzzling. In the case of Cyg X-1, the power-density spectrum (PDS) shows that most of the power emerges at Fourier frequencies corresponding to time-scales between 0.1 and 5 s (Belloni & Hasinger 1990; Van der Klis 1995). Studies of the autocorrelation function have also revealed the existence of strong correlations for lags up to ~5 s (Nolan et al. 1981; Meekins et al. 1984). These time-scales exceed by orders of magnitude the characteristic time-scales of the processes operating close to the black hole.

Another intriguing feature is the Fourier-frequency-dependent time lags between hard and soft photons (Miyamoto et al. 1988; Miyamoto et al. 1991; Cui et al. 1997; Nowak et al. 1999). As it is generally believed that Comptonization is responsible for spectral formation, these lags are sometimes attributed to the delays expected from scattering in a hot cloud. Hard photons are the result of more scattering and so emerge after, or lag behind, softer ones (Payne 1980). In order to explain lags of order ~0.1 s, a huge hot cloud of size $R \sim 10^9$–10^{10} cm is then required. Comptonization in a uniform cloud, however, produces lags independent of Fourier frequency (Miyamoto et al. 1988). This led Kazanas, Hua & Titarchuk (1997) to propose an inhomogeneous density distribution of the hot cloud. While solving one problem, however, this model raises another, more serious, one of how physically to support a cloud of such huge size for which most of the energy is at the outer boundary while all the dissipation is at the centre. Besides this, when modelling the time lags, it is also often assumed that the Compton cloud is static and it is the soft photon input that varies, contrary to what is observed (Miyamoto et al. 1991).

Miyamoto & Kitamoto (1989) were the first to propose the spectral evolution as a solution for these problems. However, in their model an ad hoc scaling between time-scales of hard and soft

★ E-mail: juri@astro.su.se (JP); acf@ast.cam.ac.uk (ACF)

pulses is assumed. Here we present a new model for the spectral variability of accreting black holes and assume that the basic unit of energy release is a flare, which defines the shortest variability time-scale. The flares are assumed to be produced from an active region in a stochastic manner, which we model as a pulse avalanche. Individual flares are assumed to move away from the disc, so that the fraction of the reprocessed soft flux that crosses the flare emission region (≡ ER) decreases with time during the life of a flare. This produces the spectral variability that causes the time delays between hard and soft photons of the order of the flare time-scale.

2 PHYSICAL PICTURE

Magnetic flares have long been considered as the source of the rapid variability of Cyg X-1 and other similar accreting black holes (Galeev, Rosner & Vaiana 1979; Haardt, Maraschi & Ghisellini 1994; Stern et al. 1995; Beloborodov 1999). Magnetic fields are amplified by the differential motion in the disc, and rise up into the corona where they reconnect and liberate their energy in a flare. Exactly how this process takes place is not clear, but there are indications that they expand and detach from the disc (see Mikic, Barnes & Schnack 1988; Amari, Luciani & Tagger 1996; Romanova et al. 1998). One expects the overall evolution time-scale of the magnetic field configuration to be of the order of the Keplerian time-scale (Romanova et al. 1998). As most of the energy in the accretion disc is dissipated within radii $\lesssim 50R_{\rm g}$ from the central black hole (here $R_{\rm g} \equiv 2GM/c^2$), these time-scales lie between ~ 1 ms and a few tenths of a second for a $M \sim 10\,{\rm M}_\odot$ black hole.

The characteristic size, R, of the magnetic loop (giving an upper limit for the size of the ER) is of the order of the turbulent cell size, equal to the half-thickness of the accretion disc (Galeev et al. 1979). For the innermost part of the accretion disc it is then $R \sim \dot{m}R_{\rm g}$ (Shakura & Sunyaev 1973), where $\dot{m} \equiv \dot{M}c^2/L_{\rm Edd} \sim 1$ in the case of Cyg X-1, and can be smaller if a large fraction of energy is dissipated above the disc, when the disc height is reduced (Svensson & Zdziarski 1994).

The reconnection of the magnetic field lines in one location can force the neighbouring field configurations into an unstable state, causing subsequent reconnections and, possibly, a long avalanche. The evolution of an individual avalanche may roughly parallel that of a solar active region (Lu & Hamilton 1991).

3 SPECTRAL EVOLUTION OF A MAGNETIC FLARE

We follow here the scenario in which magnetic fields are moving away from the underlying accretion disc in the course of the flare and estimate how the flare spectrum varies in time. We assume that a heating rate $l_{\rm h}(H)[l \equiv L\sigma_{\rm T}/(Rm_{\rm e}c^3)$ is the compactness parameter, and L is the luminosity] is a function of height, H (measured in units of the characteristic size of the ER, R), and is zero both when the ER is at the surface of the disc and when it is far away, reaching maximum in between.

The hot electrons produced by the dissipation are cooled by Comptonization of intrinsic soft photons produced in the disc by viscous dissipation (with corresponding compactness $l_{\rm s,0}$) and photons produced by reprocessing in the disc of flare radiation. In the beginning of the flare, when $l_{\rm h}$ is smaller than $l_{\rm s,0}$, the soft photons are just the average background of luminosity $l_{\rm s,0}$, and the spectrum emitted by the flare is very soft. When $l_{\rm h}$ is large, the hard X-rays produced in the ER heat up the cold disc in the vicinity of the flare, so creating extra soft photons which then dominate the cooling. The emitted spectrum defined by the geometry of the system is hard (Stern et al. 1995; Svensson 1996). The luminosity of the soft photons that crosses the ER is $l_{\rm s}(H) = l_{\rm s,0} + D(H)l_{\rm h}(H)$. The height- (and time-) dependent feedback factor, $D(H)$, determines what fraction of the hard luminosity after reprocessing in the disc returns to the ER. During the whole *feedback phase* when $l_{\rm s}(H) \gg l_{\rm s,0}$ the emission region moves away from disc thus decreasing $D(H)$. This causes a continuous increase of the Compton amplification factor, $A \equiv l_{\rm h}(H)/l_{\rm s}(H)$, and a corresponding hardening of the spectrum. In the very last phase, when intrinsic disc photons dominate cooling, the spectrum becomes soft again.

A hardening of the spectrum during the phase of maximal energy dissipation agrees well with the observation of the short time-scale spectral evolution of Cyg X-1 (Negoro et al. 1994). The luminosity in hard photons reaches a maximum later than the soft luminosity does. In order to show that the model described above can qualitatively be applied to GBHs, we have computed the temporal evolution of the flare spectrum and the time-averaged spectrum using the code of Coppi (1992) and compared it with that of Cyg X-1. For an ER of $R \lesssim R_{\rm g}$, we can assume that the spectrum is produced instantaneously (i.e. there are no time delays caused by Compton upscattering). This is a good approximation as long as the characteristic time-scale of the flare $\tau \gg R/c$. The spectral evolution can then be described as a sequence of steady states. At any given moment the spectrum is defined by three parameters: $l_{\rm s}$, $l_{\rm h}$ and the Thomson optical depth of the ER, $\tau_{\rm T}$. The Compton reflection component is also assumed to be produced in the vicinity of the flare, thus varying together with the Comptonized radiation.

The feedback factor can be parametrized as $D(H) = D_0/(1 + 3H^2)$, where the uncertainties in geometry of the ER, structure of the cold disc and the angular distribution of the flare radiation are incorporated into the factor D_0. The temperature of the disc that produces soft seed photons for Comptonization also depends on the distance of the ER from the disc:

$$T_{\rm s}(H) \approx \left\{\frac{m_{\rm e}c^3}{\sigma_{\rm T}R\sigma_{\rm SB}\pi}\left[l_{\rm s,0} + \frac{\eta l_{\rm h}(H)}{1+3H^2}\right]\right\}^{1/4}, \qquad (1)$$

and equals $T_{\rm s}(H) = 0.25[l_{\rm s,0} + \eta l_{\rm h}(H)/(1 + 3H^2)]^{1/4}$ keV for $R \sim 3 \times 10^6$ cm ($\sim R_{\rm g}$, for a 10-$\rm M_\odot$ black hole). The factor η combines the uncertainties in the angular distribution of the hard radiation and albedo for the reflection from the disc.

Assuming $l_{\rm s,0} = 0.01$, the temperature of the cold disc between flares is $T_{\rm s,0} = 80$ eV. We fix the compactness of a flare at the peak of the energy dissipation at $l_{\rm h,max} = 10$ (Haardt et al. 1994; Beloborodov 1999). As long as the ratio $l_{\rm h,max}/l_{\rm s,0}$ is large, the spectrum depends weakly on our choice of $l_{\rm h,max}$ (and $l_{\rm s,0}$), but depends strongly on the feedback and the height where most of the energy dissipation occurs. We further assume, for illustration, that the heating rate varies with time as $l_{\rm h}(t) \propto (t/\tau)^{\xi}\exp(-t/\tau)$, and the ER moves away from the disc with a constant velocity, so that $H = H_0 t/\tau$. The exact shape of the flare profile (value of ξ) does not affect any of the qualitative results. Hard spectra observed in GBHs require most dissipation to occur at a height approximately

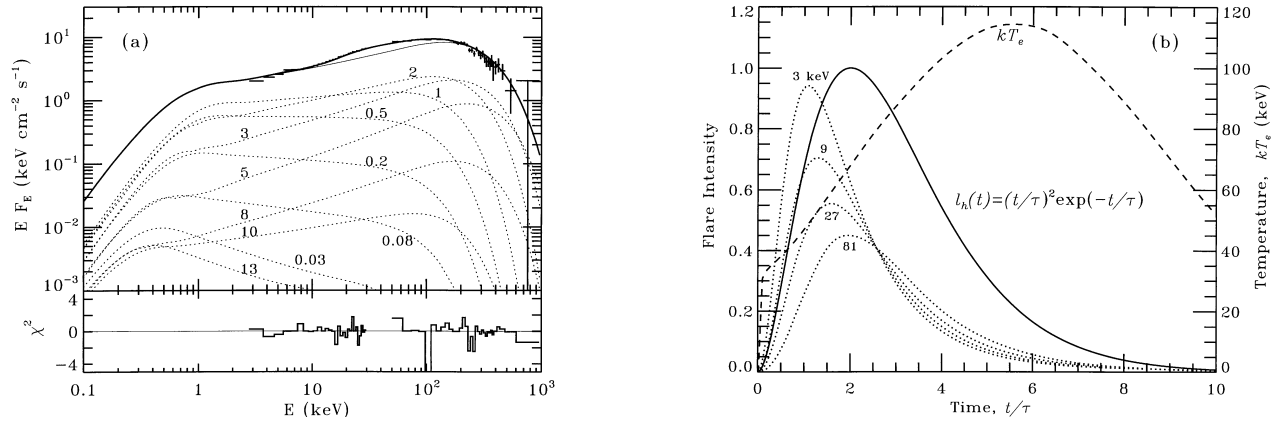

Figure 1. (a) Spectral evolution of a magnetic flare. Time-resolved spectra (without Compton reflection) are shown by dotted curves; marks are times in units of τ from the beginning of the flare. The time-averaged Comptonized spectrum plotted by a thin solid curve corresponds to the Compton amplification $A \sim 10$. The Compton reflection is computed by convolving the flare spectrum with the angle-dependent Green functions of Magdziarz & Zdziarski (1995) with inclination fixed at 30°. The time-averaged spectrum of Cyg X-1 (simultaneous *Ginga* and OSSE data from 1991 June, data set 1 in Gierliński et al. 1997) is plotted by crosses and the best-fitting flare model by a thick solid curve ($\chi^2/\mathrm{dof} = 50.0/75$). Interstellar absorption is removed when plotting the model spectrum. The best-fitting model parameters are $D_0 = 0.50^{+0.02}_{-0.02}$ and $\tau_\mathrm{T} = 1.8^{+0.1}_{-0.1}$. Here for spectral fits we use XSPEC v10 (Arnaud 1996), and the errors are given for a 90 per cent confidence interval ($\Delta\chi^2 = 2.7$). The amount of Compton reflection is $\Omega/(2\pi) = 0.30^{+0.03}_{-0.03}$, the equivalent width of the Fe line is 100 eV, and absorber column density $N_\mathrm{H} = (0.9^{+0.2}_{-0.2}) \times 10^{22}\,\mathrm{cm}^{-2}$. The contribution to χ^2 is shown at the bottom of the panel. (b) The flare light curves (in arbitrary units) at 3, 9, 27 and 81 keV are shown by dotted curves; the heating rate, $l_\mathrm{h}(t)$, by a solid curve. The temperature of the ER, kT_e (dashed curve), peaks at the time when Compton amplification $A(t)$ is largest. Pulses at different energies are almost self-similar, i.e. they can be represented by the same $(t/\tau_E)^2 \exp(-t/\tau_E)$ law with time constants at photon energy E approximately following a logarithmic dependence, $\tau_E \approx \tau[1 + (1/8)\ln(E/E_\mathrm{p})]$, where τ is the time constant of the energy dissipation $l_\mathrm{h}(t)$ and E_p is the photon energy where EF_E peaks. Thus the delay between photons of energies E and E_0 is $\Delta t \approx (\tau/4)\ln(E/E_0)$.

equal to the size of the ER (Svensson 1996) if the X-ray emission is isotropic (i.e. $\eta \sim 1/2$). Thus we take $\xi = 2$ (ad hoc), $H_0 = 1/\xi = 1/2$, $\eta = 1/2$, and fit D_0. Altogether, we have only two free parameters, D_0, and the Thomson optical depth, τ_T, that determine the flare spectrum. To be specific, D_0 determines the slope of the spectrum, while τ_T determines the electron temperature and the spectral cut-off. We note that parameters H_0 and D_0 are strongly correlated, i.e., if one decreases H_0, the same spectrum can be produced decreasing D_0. In the case of a thermal plasma (assumed here) and $l \sim 10$, the contribution from the $\mathrm{e}^\pm$ pairs is negligible for the spectrum observed in Cyg X-1.

With these assumptions, we compute the spectral evolution of the flare (see Fig. 1a) and find that the time-averaged spectrum of the flare gives a very good fit to the data of Cyg X-1. If there were anisotropy breaks in the time-resolved spectra (Stern et al. 1995) because of the anisotropy of the soft photon injection into the ER (neglected here), the spectral evolution would smooth them out. In the isotropic case, the time-averaged Comptonized spectrum is slightly concave and generally cannot be described by a Comptonized spectrum with a fixed optical depth and temperature.

From the spectral evolution we can compute the flare light curves in various energy bands (Fig. 1b). Owing to the soft-to-hard evolution, soft photons come first, while the hard photon flux (at $\sim$100 keV) follows the evolution of the heating rate and peaks later. This delay of hard photons relative to soft ones causes time lags to appear in the composite light curves from an ensemble of flares.

4 THE PULSE AVALANCHE MODEL

GBHs as well as many other complex physical systems often show $1/f$ noise in their PDS (Press 1978). There is no accepted theory for the origin of this noise. One possibility is that a system develops into a self-organized critical state (Bak, Tang & Wiesenfeld 1987; Mineshige, Ouchi & Nishimori 1994; Mineshige & Negoro 1999). In general, correlations between signals (flares) of very different time-scales are required. We model such correlations using a version of a simple stochastic pulse avalanche model from Stern & Svensson (1996), originally invented to describe the temporal characteristics of gamma-ray bursts.

We assume that some flares occur spontaneously according to a Poisson distribution with a mean rate of λ flares per second (as in the shot noise model; Terrel 1972). All flares can stimulate the production of flares, the number following a Poisson distribution of mean number μ. Each spontaneous flare ($\equiv$ pulse) gives rise to a 'pulse avalanche', and the whole light curve is produced by an overlap of such avalanches. Stimulated pulses are delayed from the stimulating pulse by a time Δt, which is drawn from a Poisson distribution of mean $\alpha\tau_1$, where α is a delay parameter and τ_1 is the time constant of the stimulating pulse. This could be interpreted as a 'reservoir' effect (Begelman & de Kool 1991). A long (i.e. energetic) flare would drain the system of a larger amount of stored energy, which results in a longer time being required to store up enough energy for a subsequent flare. The presence of such reservoirs is also supported by the observations (Negoro et al. 1995). The time constant of energy dissipation, τ, for all pulses (spontaneous and stimulated) is assumed to be distributed according to a power law, $\rho(\tau) \propto \tau^{-p}$ between τ_min and τ_max. We assume that all pulses have the same shape and amplitude as shown in Fig. 1 and differ only in time constant, τ. In total we have six parameters: λ, μ, α, τ_min, τ_max and p, but it is quite easy to navigate in the parameter space. In order to describe the role of the parameters, we discuss how each of them influences the PDS of a simulated light curve.

5 RESULTS OF SIMULATIONS

We assume that all flares produce the time-resolved spectra and energy-dependent pulses shown in Figs 1(a) and (b). The variability and interaction between individual flares are described by a pulse avalanche model. Thus we are now able to simulate the light curves (Fig. 2a). The model parameters ($\lambda = 45$; $\mu = 0.8$; $\alpha = 7$; $p = 1$; $\tau_{\rm min} = 1$ ms; $\tau_{\rm max} = 0.15$ s) were selected to match a typical PDS of Cyg X-1, which can be described as a doubly broken power law: a flat, white noise, part f^0, below some frequency $f_{\rm flat}$; flicker noise, f^{-1}, between $f_{\rm flat}$ and $f_{\rm br}$; and 'red' noise, $f^{-\beta}$ with $\beta \sim 1.5$–2, above $f_{\rm br}$. Normally, $f_{\rm flat} \sim 0.05$–0.1 Hz and $f_{\rm br} \sim 2$ Hz (Fig. 2b; Belloni & Hasinger 1990; Nowak et al. 1999).

We identify $f_{\rm br}$ with the longest time-scale of an individual flare $\tau_{\rm max} \approx 1/(2\pi f_{\rm br})$. We note that flares of duration τ, with the dissipation varying as $(t/\tau)^{\xi}\exp(-t/\tau)$, produce a PDS $\propto [(2\pi f)^2 + (1/\tau)^2]^{-(\xi+1)}$ decaying as $f^{-2(\xi+1)}$ at high frequencies and giving contributions to the total PDS in a very narrow frequency interval around $f \sim 1/(2\pi\tau) > f_{\rm br}$, so that an actual value of ξ affects none of the qualitative results. The absence of a break at $f \sim 1/(2\pi\tau_{\rm min})$, corresponding to the minimum time-scale, in the Cyg X-1 data, constrains $\tau_{\rm min} \lesssim 2$ ms. The flare time-scales can be related to the Keplerian time-scales at radii between the innermost stable orbit and $\sim 30R_{\rm g}$. The low-frequency break $f_{\rm flat} \sim 0.1$ Hz is related to the duration of the avalanche: $\sim \alpha\bar{\tau}\mu/(1-\mu) \sim 1$ s, where $\bar{\tau}$ is the time-scale of the flare averaged over $\rho(\tau)$. The power-law index p of the time-scale distribution is related to the slope, $\beta = 3 - p$, of the PDS at $f > f_{\rm br}$ (e.g. Lochner, Swank & Szymkowiak 1991). The hardening of the PDS with photon energy (Nowak et al. 1999) is not reproduced by our model, which predicts the same β for all energies.

Parameters α and μ determine the duration of the avalanches, which, in turn, define the length and slope of the flicker noise part of the PDS, where most of the power emerges. The $1/f$ part of the PDS is present for a very broad range of parameters ($4 \lesssim \alpha \lesssim 10$ and $0.6 \lesssim \mu \lesssim 0.9$). The larger α and μ, the longer the avalanches, the smaller $f_{\rm flat}$, and the larger the fractional root-mean-square (rms) amplitude of the variability (i.e. the normalization of the PDS). Increases in both α and μ can thus account for the observed anticorrelation between $f_{\rm flat}$ and the rms amplitude (Belloni & Hasinger 1990). The average number of spontaneous pulses, λ, is a trivial parameter which defines the rms amplitude, rms $\propto 1/\sqrt{\lambda}$ ($\sim$30 per cent in the case of Cyg X-1:

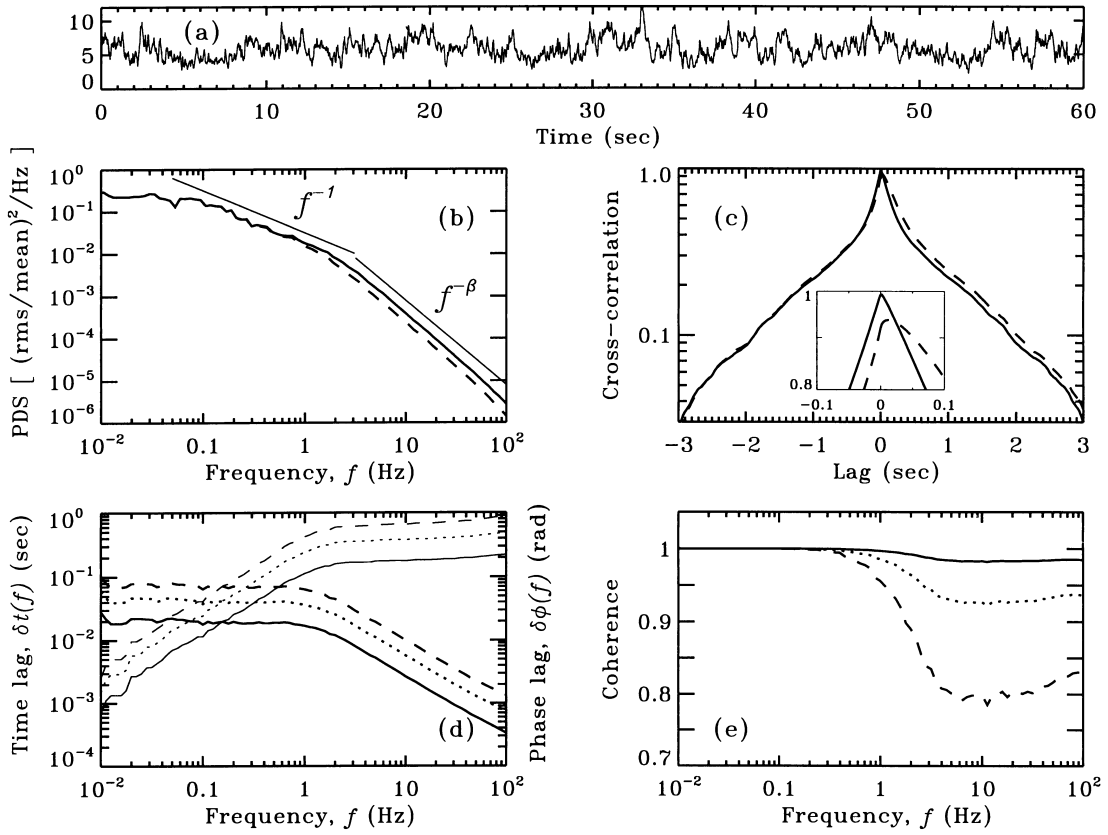

Figure 2. (a) An example of a simulated light curve at 3 keV. (b) The power-density spectrum (PDS) at 3 keV (solid curve) and 27 keV (dashed). For a very broad range of parameters, the PDS can be represented as a doubly broken power law. The slope β at high frequencies is related to the slope of the time constant distribution, $\beta = 3 - p$ (in our case $\beta = 2$). (c) Normalized cross-correlation functions for 9 keV (solid curve) and 81 keV (dashed curve) versus 3 keV. The 9-keV CCF peaks at a lag $< 10^{-3}$ s and is almost symmetric; for higher energies, the peak of the CCFs shifts more towards positive lags and the CCFs become more asymmetric. The insert shows CCF behaviour near the peak. (d) Time lags, $\delta t(f) = \delta\phi(f)/(2\pi f)$ (thick curves), and phase lags, $\delta\phi(f)$ (thin curves), for various energy bands: 9 keV (solid), 27 keV (dotted), and 81 keV (dashed) versus 3 keV. The maximum time lags can be approximately described by $\delta t_{\rm max} \approx (\tau_{\rm max}/8)\ln(E/E_0)$, where E and E_0 are the corresponding energies and $\tau_{\rm max}$ is the maximum flare time-scale. As time lags are proportional to the time-scale of the flare (see Fig. 1b), $\delta t(f) \propto \tau \approx 1/(2\pi f)$ (i.e. phase lags are almost constant) at frequencies $f > f_{\rm br}$ related to individual flares. (e) Coherence functions, with the same definitions as (d). Note the different behaviour at frequencies below and above $f_{\rm br}$ and the decrease of the frequency at which loss of coherence occurs when E increases.

Belloni & Hasinger 1990;Van der Klis 1995). The rms amplitude decreases slightly with photon energy, in agreement with the data (Nowak et al. 1999).

Besides the PDS, we also compute the normalized cross-correlation functions (CCFs), time/phase lags and coherence functions. The CCFs (Fig. 2c) are slightly asymmetric (see e.g. Nolan et al. 1981) and peak at almost zero lags. They are well described by a stretched exponential law $\exp(-|t/t_0|^{\nu})$ with the index $\nu \sim 1/2$ and $t_0 \sim 0.4$ s within $|t| \lesssim 2$ s. A similar stretched exponential behaviour is found in the autocorrelation function of gamma-ray bursts (Stern & Svensson 1996) and is known to describe some characteristics of turbulence (see e.g. Ching 1991).

Time lags, $\delta t(f)$ (Fig. 2d), decay approximately as $1/f$ above $f_{\rm br}$, where individual pulses dominate the PDS:

$$\delta t(f) \approx \delta t_{\rm max} \times \begin{cases} 1, & f < f_{\rm br}, \\ (f/f_{\rm br})^{-1}, & f > f_{\rm br}, \end{cases} \qquad (2)$$

where $\delta t_{\rm max} \approx (\tau_{\rm max}/8) \times \ln(E/E_0)$ is the maximum achievable time lag (here E and E_0 are the corresponding photon energies). As time lags are proportional to the time-scale of the pulse, $\tau \approx 1/(2\pi f)$, which gives the contribution to the PDS at frequency f, they are smaller at higher frequencies. The maximum lag $\delta t_{\rm max}$ is a factor of 2 smaller than expected in a shot noise model with a fixed time constant $\tau_{\rm max}$ (see Fig. 1b), as a result of averaging over different time-scales. A wide distribution of time-scales of the individual flares ensures that there are non-negligible time lags and, at the same time, CCFs peaking at almost zero lags. The logarithmic dependence of time lags on E is consistent with the observations of Cyg X-1 and other GBHs (e.g. Cui 1999; Nowak et al. 1999). An amusing fact is that a similar logarithmic relation holds for Comptonization in a static cloud (Payne 1980), where higher energy photons, which spend more time in the medium, lag behind softer ones. The data for Cyg X-1 (Nowak et al. 1999) show more complicated behaviour of the time-lags with Fourier frequency. Our model reproduces successfully a $1/f$ dependence above $\sim$1 Hz and a 'shoulder' at $\sim$0.5–1 Hz. A break in the time lag at $\sim$0.5 Hz is not reproduced by the model. In Section 6, we speculate on a possible origin for such a break.

The coherence function (cf. Bendat & Piersol 1986; Vaughan & Nowak 1997) is close to unity (Fig. 2e), because the light curves at different energies are almost perfectly synchronized. Deviations from unity become visible at frequencies where individual pulses contribute to the PDS ($f \gtrsim f_{\rm br} \sim 1$ Hz) and large E, which is consistent with the data for Cyg X-1 at $f \lesssim 10$ Hz (Nowak et al. 1999), but not as strong as might be seen for $f \gtrsim 10$ Hz (although we note that those data are especially prone to systematic uncertainties that were not fully considered by Nowak et al.). The larger E, the smaller the coherence function and the smaller the Fourier frequency where loss of coherence starts. The same behaviour is expected for any energy-dependent shot noise model.

The parameter ξ of the individual pulse profile affects the time delays between photons of different energies. This, in turn, affects the time lags and the coherence function in such a way that the larger ξ, the larger the coherence and the smaller the time lags. Changing α, μ, p or λ in the pulse avalanche model hardly has *any* influence on the dependence of the time lags and coherence function on frequency. We note that changing $\tau_{\rm max}$ affects the break in the PDS, $f_{\rm br} \sim 1/(2\pi\tau_{\rm max})$, and correspondingly changes the frequency where loss of coherence occurs. The maximum achievable time lag is also affected, $\delta t_{\rm max} \propto \tau_{\rm max}$.

The total averaged luminosity of the system, $L = L_{\rm h,max}\bar{\tau}\lambda e^2/[2(1-\mu)]$ erg s^{-1}, determines the average peak luminosity of individual flares, $L_{\rm h,max}$. We find $L_{\rm h,max} \sim 1.6 \times 10^{36}$ erg s^{-1} taking the Cyg X-1 luminosity $L = 4 \times 10^{37}$ erg s^{-1} (Gierliński et al. 1997). The peak compactness of the flare is then $l_{\rm h,max} \approx 15(R/R_{\rm g})^{-1}$. This confirms a posteriori our choice of $l_{\rm h,max}$ in Section 3. There are $\lambda\bar{\tau}/(1-\mu) \sim 7$ flares active at any given time. The total energy dissipated during the flare $E_{\rm fl} \sim L_{\rm h,max}\bar{\tau}$ constrains the magnetic field in the flaring region to be of the order of $B \sim \sqrt{6E_{\rm fl}/R^3} \sim 10^8$ G.

6 DISCUSSION

The model we present can be developed in numerous ways. We assumed that the spectral evolution occurs because of the inflation of the magnetic loop configuration. This is, of course, not a unique possibility. A number of other scenarios can produce similar behaviour (see Poutanen & Fabian 1999). Another assumption, that the spectrum is formed instantaneously, is no longer valid for short flares, $\tau \lesssim$ a few R/c ($\sim$1 ms in our case, with a more stringent limit for higher observed photon energy), because delays resulting from Compton upscattering and production of reprocessed soft photons then have to be incorporated. The delays in the production of soft (reprocessed) photons can make the Comptonized spectrum hard in the beginning of the flare and soft later, producing *negative* lags at $f \gtrsim 50$ Hz.

In our model, the longer flares appear to be very smooth, while, in reality, they can consist of a train of correlated, much shorter, flares. This effect can also significantly affect the PDS behaviour at high frequencies (possibly even accounting for the hardening of the PDS with photon energy; Nowak et al. 1999).

Another simplification is that we assumed that Compton reflection is produced in the vicinity of the flare. However, it is possible that some fraction of the hard radiation is reflected, e.g. from the outer disc, the wind, or the companion star. This would cause a suppression of the variability of this component at short time-scales (acting as a low-pass filter) and produce additional time lags independent of Fourier frequency. A break in the time lag–Fourier frequency relation should then appear for energies where Compton reflection is not negligible (e.g. comparing $E \gtrsim 7$ keV and $E \lesssim 2$ keV channels), and it can be used to determine the distance of the reflector from the X-ray source. We propose that the break in the time lags at $f \sim 0.5$ Hz observed in Cyg X-1 (Nowak et al. 1999) can be a consequence of this effect.

An important issue is the small amplitude of Compton reflection seen in Cyg X-1 and other GBHs in their hard state (Ebisawa et al. 1996; Gierliński et al. 1997; Zdziarski et al. 1998), $\Omega/(2\pi) \approx 0.3$. These observations have been interpreted as an absence of reflecting material in the direct vicinity of the X-ray source (cf. Dove et al. 1997; Poutanen, Krolik & Ryde 1997). In the present model, we explicitly assume that cold material exists in the vicinity of the flare and produces soft photons by reprocessing hard X-ray radiation. Possible solutions include the following alternatives: (i) the cold disc is disrupted into a number of cold filaments that produce enough seed soft photons for Comptonization, but have too small a covering factor to produce visible Compton reflection (Lightman 1974; Krolik 1998; Poutanen 1999; Zdziarski et al. 1998); (ii) there is bulk motion directed away from the disc and more flare radiation is beamed toward the observer than the disc (Beloborodov 1999); or (iii) the disc is highly ionized (Ross, Fabian & Young 1999).

An interesting question is why the time lags in the soft state of Cyg X-1 are smaller than those in the hard state (Cui et al. 1997). We can suggest at least two reasons. First, because the soft state spectrum is *softer*, the amplitude of the spectral evolution is much smaller. Secondly, if in the soft state X/γ-rays are produced only within $\sim 10 R_{\rm g}$ from the black hole, the dynamical time-scales are on average smaller, causing smaller lags.

7 SUMMARY

We have presented a model for the short time-scale spectral variability of accreting black holes, and showed using Cyg X-1 that it is able to describe time-averaged spectra as well as the general behaviour of temporal characteristics such as power-density spectra, time/phase lags and coherence function. We based our *spectral* model on the fact that magnetic loops have a tendency to inflate and detach from the accretion disc. The corresponding decrease of the feedback from the cold disc causes the soft-to-hard evolution of the flare spectrum, which is the reason for time lags between hard and soft photons. We assumed that all properties of the flares scale with their time-scale, τ. This produces the time delays between hard and soft photons in an individual flare, also scaling with τ. In their turn, the time lags from an ensemble of flares of different duration show an $1/f$ dependence on the Fourier frequency.

The model for the *temporal variability* is based on a pulse avalanche model where flares can, with some probability, trigger other flares. The duration of the avalanches, which are the result of this interaction, determines the Fourier frequencies at which most of the power emerges.

We identified the break in the PDS at $f_{\rm br}$ with the maximum time-scale of an individual flare $\tau_{\rm max} \approx 1/(2\pi f_{\rm br})$ and pointed out that statistical properties are very different at $f < f_{\rm br}$ and $f > f_{\rm br}$. Deviation from unity of the coherence function and the break in the time/phase lag spectrum occur also close to $f_{\rm br}$. The PDS, time/phase lags and coherence at $f > f_{\rm br}$ are related to the properties of the individual flares, while the behaviour at $f < f_{\rm br}$ is a property of a stochastic process. Our model predicts that variations of $f_{\rm br}$ in the PDS should be accompanied by corresponding changes in the time/phase lag and coherence spectra.

The success of the model in reproducing most of the spectral and temporal properties of Cyg X-1 supports the point of view in which X/γ-rays are produced in localized hot regions (magnetic flares) that interact with each other. We expect that this model may also be useful when analysing data from other accreting objects such as active galactic nuclei and weakly magnetized neutron stars.

ACKNOWLEDGMENTS

We are grateful to Boris Stern for the original version of the pulse avalanche model and to Paolo Coppi for the EQPAIR code. Helpful discussions with the participants of the workshop on High Energy Processes in Accreting Black Holes and useful suggestions of the anonymous referee are acknowledged. JP is grateful to the Institute of Astronomy for their hospitality during his visit. His work was supported by the Swedish Natural Science Research Council and the Anna-Greta and Holger Crafoord Fund. ACF thanks the Royal Society for support.

REFERENCES

Amari T., Luciani J. F., Tagger M., 1996, A&A, 306, 913
Arnaud K. A., 1996, in Jacoby G. H., Barnes J., eds, ASP Conf. Ser. Vol. 101. Astron. Soc. Pac., San Francisco, p. 17
Bak P., Tang C., Wiesenfeld K., 1987, Phys. Rev. Lett., 59, 381
Begelman M. C., de Kool M., 1991, in Miller H. R., Wiita P. J., eds, Variability of Active Galactic Nuclei. Cambridge Univ. Press, Cambridge, p. 198
Belloni T., Hasinger G., 1990, A&A, 227, L33
Beloborodov A. M., 1999, ApJ, 510, L123
Bendat J. S., Piersol A. G., 1986, Random Data: Analysis and Measurement Procedures, Wiley, New York
Ching E., 1991, Phys. Rev. A, 44, 3622
Coppi P. S., 1992, MNRAS, 258, 657
Cui W., 1999, in Poutanen J., Svensson R., eds, ASP Conf. Ser. Vol. 161. Astron. Soc. Pac., San Francisco, p. 97
Cui W., Zhang S. N., Focke W., Swank J. H., 1997, ApJ, 484, 383
Dove J. B., Wilms J., Maisack M., Begelman M. C., 1997, ApJ, 487, 759
Ebisawa K., Ueda Y., Inoue H., Tanaka Y., White N. E., 1996, ApJ, 467, 419
Galeev A. A., Rosner R., Vaiana G. S., 1979, ApJ, 229, 318
Gierliński M., Zdziarski A. A., Done C., Johnson W. N., Ebisawa K., Ueda Y., Haardt F., Phlips B. F., 1997, MNRAS, 288, 958
Haardt F., Maraschi L., Ghisellini G., 1994, ApJ, 432, L95
Kazanas D., Hua X. M., Titarchuk L., 1997, ApJ, 480, 735
Krolik J. H., 1998, ApJ, 498, L13
Lightman A. P., 1974, ApJ, 194, 429
Lochner J. C., Swank J. H., Szymkowiak A. E., 1991, ApJ, 376, 295
Lu E. T., Hamilton R. J., 1991, ApJ, 380, L89
Magdziarz P., Zdziarski A. A., 1995, MNRAS, 273, 837
Meekins J. F., Wood K. S., Hedler R. L., Byram E. T., Yeutis D. J., Chubb T. A., Friedman H., 1984, ApJ, 278, 288
Mikic Z., Barnes D. C., Schnack D. D., 1988, ApJ, 328, 830
Mineshige S., Negoro H., 1999, in Poutanen J., Svensson R., eds, ASP Conf. Ser. Vol. 161. Astron. Soc. Pac., San Francisco, p. 113
Mineshige S., Ouchi N. B., Nishimori H., 1994, PASJ, 46, 97
Miyamoto S., Kitamoto S., 1989, Nat, 342, 773
Miyamoto S., Kitamoto S., Mitsuda K., Dotani T., 1988, Nat, 336, 450
Miyamoto S., Kimura K., Kitamoto S., Dotani T., Ebisawa K., 1991, ApJ, 383, 784
Negoro H., Miyamoto S., Kitamoto S., 1994, ApJ, 423, L127
Negoro H., Kitamoto S., Takeuchi M., Mineshige S., 1995, ApJ, 452, L49
Nolan P. L. et al., 1981, ApJ, 246, 494
Nowak M. A., Vaughan B. A., Wilms J., Dove J. B., Begelman M. C., 1999, ApJ, 510, 874
Payne D. G., 1980, ApJ, 237, 951
Poutanen J., 1999, in Abramowicz M. A., Björnsson G., Pringle J. E., eds, Theory of Black Hole Accretion Discs. Cambridge Univ. Press, Cambridge, p. 100
Poutanen J., Fabian A. C., 1999, in Poutanen J., Svensson R., eds, ASP Conf. Ser. Vol. 161. Astron. Soc. Pac., San Francisco, p. 135
Poutanen J., Krolik J. H., Ryde F., 1997, MNRAS, 292, L21
Press W. H., 1978, Comm. Astrophys., 7, 103
Romanova M. M., Ustyugova G. V., Koldoba A. V., Chechetkin V. M., Lovelace R. V. E., 1998, ApJ, 500, 703
Ross R. R., Fabian A. C., Young A. J., 1999, MNRAS, 306, 461
Shakura N. I., Sunyaev R. A., 1973, A&A, 24, 337
Shapiro S. L., Lightman A. P., Eardley D. N., 1976, ApJ, 204, 187
Stern B. E., Svensson R., 1996, ApJ, 469, L109
Stern B. E., Poutanen J., Svensson R., Sikora M., Begelman M. C., 1995, ApJ, 449, L13
Sunyaev R. A., Trümper J., 1979, Nat, 279, 506
Svensson R., 1996, A&AS, 120, 475

Svensson R., Zdziarski A. A., 1994, ApJ, 436, 599
Terrel N. J. Jr, 1972, ApJ, 174, L35
Van der Klis M., 1995, in Lewin W. H. G., van Paradijs J., van den Heuvel E. P. J., eds, Cambridge Astrophys. Ser. Vol. 26, X-ray Binaries. Cambridge Univ. Press, Cambridge, p. 252
Vaughan B. A., Nowak M. A., 1997, ApJ, 474, L43
Zdziarski A. A., Poutanen J., Mikołajewska J., Gierliński M., Ebisawa K., Johnson W. N., 1998, MNRAS, 301, 435

This paper has been typeset from a TEX/LATEX file prepared by the author.